Developmental Cognitive Neuroscience 62 (2023) 101265

Contents lists available at ScienceDirect

Developmental Cognitive Neuroscience

journal homepage: www.elsevier.com/locate/dcn

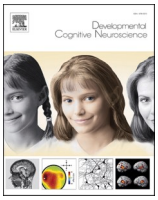

Individual differences in delay discounting are associated with dorsal prefrontal cortex connectivity in children, adolescents, and adults

Kahini Mehta [a,b], Adam Pines [a,b], Azeez Adebimpe [a,b], Bart Larsen [a,b], Danielle S. Bassett [c,d,h,i,j], Monica E. Calkins [b], Erica B. Baller [a,b], Martin Gell [a,k,l], Lauren M. Patrick [f], Golia Shafiei [a,b], Raquel E. Gur [b,g,h], Ruben C. Gur [b,g,h], David R. Roalf [b], Daniel Romer [e], Daniel H. Wolf [b], Joseph W. Kable [f], Theodore D. Satterthwaite [a,b,g,*,1,2]

[a] Lifespan Informatics and Neuroimaging Center (PennLINC), Perelman School of Medicine, University of Pennsylvania, Philadelphia, PA 19104, USA
[b] Department of Psychiatry, University of Pennsylvania, Philadelphia, PA, 19104, USA
[c] Department of Bioengineering, School of Engineering and Applied Science, University of Pennsylvania, PA 19104, USA
[d] Department of Electrical & Systems Engineering, University of Pennsylvania, PA 19104, USA
[e] Annenberg Public Policy Center, University of Pennsylvania, Philadelphia, PA 19104, USA
[f] Department of Psychology, University of Pennsylvania, Philadelphia, PA 19104, USA
[g] Penn/CHOP Lifespan Brain Institute, University of Pennsylvania, Philadelphia, PA 19104, USA
[h] Department of Neurology, University of Pennsylvania, Philadelphia, PA, 19104, USA
[i] Department of Physics & Astronomy, University of Pennsylvania, Philadelphia, PA, 19104, USA
[j] Santa Fe Institute, Santa Fe, NM, 87051, USA
[k] Department of Psychiatry, Psychotherapy and Psychosomatics, Medical Faculty, RWTH Aachen University, Aachen, Germany
[l] Institute of Neuroscience and Medicine (INM-7: Brain & Behaviour), Research Centre Jülich, Jülich, Germany

ARTICLE INFO

Keywords:
Delay discounting
Youth
FMRI
Functional connectivity
DMN
Resting-state

ABSTRACT

Delay discounting is a measure of impulsive choice relevant in adolescence as it predicts many real-life outcomes, including obesity and academic achievement. However, resting-state functional networks underlying individual differences in delay discounting during youth remain incompletely described. Here we investigate the association between multivariate patterns of functional connectivity and individual differences in impulsive choice in a large sample of children, adolescents, and adults. A total of 293 participants (9–23 years) completed a delay discounting task and underwent 3T resting-state fMRI. A connectome-wide analysis using multivariate distance-based matrix regression was used to examine whole-brain relationships between delay discounting and functional connectivity. These analyses revealed that individual differences in delay discounting were associated with patterns of connectivity emanating from the left dorsal prefrontal cortex, a default mode network hub. Greater delay discounting was associated with greater functional connectivity between the dorsal prefrontal cortex and other default mode network regions, but reduced connectivity with regions in the dorsal and ventral attention networks. These results suggest delay discounting in children, adolescents, and adults is associated with individual differences in relationships both within the default mode network and between the default mode and networks involved in attentional and cognitive control.

1. Introduction

Delay discounting (DD) is a measure of impulsive decision-making (Madden et al., 2003) that refers to preference for a smaller reward sooner rather than a larger reward later (Bickel et al., 2012; Epstein et al., 2010). DD predicts many real-life outcomes, such as academic achievement and social functioning (Hirsh et al., 2008; Mahalingam et al., 2016). Additionally, DD is considered an important trans-diagnostic behavior that is altered across multiple clinical disorders that are characterized by impulsive decisions, including substance misuse,

* Correspondence to: Penn Lifespan Informatics and Neuroimaging Center (PennLINC), Perelman School of Medicine, University of Pennsylvania, USA.
E-mail address: sattertt@pennmedicine.upenn.edu (T.D. Satterthwaite).
[1] **Mailing address:** Richards Medical Labs, 5th floor, 3700 Hamilton Walk, Philadelphia, PA 19104, USA.
[2] www.pennlinc.io

https://doi.org/10.1016/j.dcn.2023.101265
Received 25 January 2023; Received in revised form 24 May 2023; Accepted 11 June 2023
Available online 12 June 2023

schizophrenia, and attention-deficit hyperactivity disorder (ADHD; Amlung et al., 2019; Chase and Hogarth, 2011; Weller et al., 2014; Ortiz et al., 2015; Lempert et al., 2019). A better understanding of the mechanisms of DD could thus inform decisions regarding early interventions for certain disorders, particularly in at-risk adolescents. However, studies that link resting-state brain networks defined using functional connectivity (FC) to DD in youth remain sparse. Here, we sought to understand how DD is related to individual differences in resting-state functional brain networks in a large sample of children, adolescents, and adults.

Many studies have used task-based fMRI to uncover the brain regions engaged during DD, especially key regions involved in reward valuation such as the ventral striatum and hubs of the default mode network (DMN) such as the ventromedial prefrontal cortex (vmPFC) and posterior cingulate cortex (PCC; Schüller et al., 2019; Souther et al., 2022; Kable and Glimcher, 2007; Peters and Büchel, 2010). A related but distinct approach links DD to FC at rest instead of task-based responses. Work using resting-state fMRI and FC is motivated in part by behavioral data that has suggested DD is a stable trait that varies among individuals and is heritable (Kirby, 2009). FC has previously proven predictive of individual personality traits and has also been used successfully to identify neural correlates of DD (Kable and Levy, 2015). Studies of individual differences in FC related to DD often use a network-based framework, which is supported by prior research suggesting that DD relies upon interactions among multiple brain networks during rest (Chen et al., 2017). Specifically, prior work in adults has linked impulsive choice during DD to individual differences in connectivity in regions involved in reward and valuation such as the striatum, vmPFC and PCC (Kable and Levy, 2015; Li et al., 2013; Calluso et al., 2015). Work in adults has also found that connectivity between the DMN and cognitive control networks such as the ventral attention (VAN) and cingulo-opercular networks is predictive of DD– increased FC between these typically anticorrelated networks could disrupt cognitive control and impact decisions on DD tasks (Chen et al., 2018). This is consistent with the idea of a role for top-down attentional/cognitive control in delay of gratification, as indicated in previous work (Hare et al., 2014; Mischel et al., 1989).

While there have been fewer studies of children and adolescents, prior work investigating ADHD has also related individual differences in DD to connectivity in regions important for valuation, such as the nucleus accumbens (Costa Dias et al., 2013). Similarly, work in both typically developing populations and children with ADHD indicates that cognitive control regions such as the dorsolateral prefrontal cortex (dlPFC) are related to DD in adolescents (Wang et al., 2017; Rosch et al., 2018). However, results from prior work in adolescents are for the most part heterogeneous, which may be driven by two factors. First, many studies of DD and resting-state functional networks in pediatric samples have been small, increasing the risk of type I error and reducing the likelihood of replicable results (Marek et al., 2022; Button et al., 2013). Second, many studies have related DD to FC among a specific set of regions or limited set of networks, rather than evaluating the complete functional connectome at rest. As DD is a complex cognitive process that involves multiple brain networks, such studies may not capture important differences in connectivity that are distributed across the cortex (Chen et al., 2017).

Accordingly, here we investigated how individual differences in DD are associated with connectome-wide differences in patterns of FC during adolescence. We capitalized on a large sample of 293 children, adolescents, and adults imaged as part of the Philadelphia Neurodevelopmental Cohort (Satterthwaite et al., 2014; Satterthwaite et al., 2016) who completed a DD task and resting-state fMRI. We conducted a connectome-wide association study (CWAS) to reveal DD-associated differences in the multivariate pattern of connectivity at each location in the brain (Shehzad et al., 2014; Sharma et al., 2017). While CWAS is a data-driven approach, we sought to test the hypothesis that individual differences in DD would be linked to connectivity in regions of both the DMN and networks involved in attentional control.

2. Methods

2.1. Participants

This study considers participants who completed both neuroimaging and a DD task as part of the Philadelphia Neurodevelopmental Cohort (PNC; Satterthwaite et al., 2014); this sample largely overlaps with a previous report linking DD to individual differences in brain structure (Pehlivanova et al., 2018). Of the 1601 participants who completed neuroimaging as part of the PNC, 453 participants completed a behavioral DD task outside of neuroimaging sessions and were thus eligible for further analyses. Of these, n = 2 did not meet the quality control criteria for behavioral data (Pehlivanova et al., 2018; see below). Further, 21 participants were excluded for the following reasons: health conditions that could impact brain structure (n = 19), scanning performed 12 months from the time of DD testing (n = 1), and missing imaging data (n = 1). An additional 137 participants were excluded due to poor quality scans, as described in the *Image quality assurance* section. Thus, a total of 293 participants (ages 9–23 years; M = 17.18 years, SD = 3.10 years; 156 females, 137 males) formed the sample for our analyses after quality control.

2.2. Ethics

This study received approval from the institutional review boards at the University of Pennsylvania and Children's Hospital of Philadelphia. All adult participants provided informed consent. For minors, parents or guardians provided informed consent and the minor provided assent.

2.3. DD task

The DD task consisted of 34 self-paced questions where the participant chose between a smaller amount of money available immediately or a larger amount available after a delay (Senecal et al., 2012; Pehlivanova et al., 2018). The smaller, immediate rewards ranged from $10 to $34, and the larger, delayed rewards were fixed at $25, $30, or $35 with equal frequency. Delays ranged from 1 to 171 days. Trials and task procedures were identical in content and order for all participants. The DD task was administered as part of an hour-long web-based battery of neurocognitive tests as part of a procedure used previously, on a separate day from the imaging session (Gur et al., 2010; Gur et al., 2012). The mean interval between the DD task and imaging was 0.44 months with a standard deviation of 1.06 months.

Discount rates from the DD task were calculated with hyperbolic discounting model of the form:

$$V = A/(1+kD),$$

where V is the subjective value of the delayed reward, A is the amount of the delayed reward, D is the delay in days, and k is the subject-specific discount rate (Mazur, 1987; Kable and Glimcher, 2010). As in previous work, the *fmincon* optimization algorithm in MATLAB (MathWorks) was used to estimate the best fitting k from each participant's choice data, assuming that choices were a logistic function of Vs (Senecal et al., 2012; Pehlivanova et al., 2018). A higher k value indicates steeper discounting of delayed rewards and thus more impulsive choices. As the distribution of estimated k parameters is right-skewed, we applied a log-transform ($\log(k)$) before further analysis. The mean value of $\log(k)$ was −3.47 with a standard deviation of 1.49 (see Fig. S1). Quality assurance of DD data was conducted as described previously: each participant's responses were fit using a logistic regression model, with predictors including the immediate amount, delayed amount, delay, their respective squared terms, and two-way interaction terms (Pehlivanova et al., 2018). The goodness of fit of this model was assessed using

the coefficient of discrimination (Tjur, 2009); a value less than 0.20 indicated nearly random choices and resulted in exclusion (Pehlivanova et al., 2018).

We evaluated associations between log(k) and demographic variables. As prior (Pehlivanova et al., 2018), we used a general additive model with penalized splines to evaluate both linear and non-linear associations of age and DD.

2.4. Image acquisition

All MRI scans were acquired using the same 3 T Siemens (Erlangen, Germany) Tim Trio whole-body scanner and 32-channel head coil at the Hospital of the University of Pennsylvania. Image acquisition protocols are described in detail in previous work (Satterthwaite et al., 2014). Briefly, the magnetization-prepared, rapid acquisition gradient-echo T1-weighted (MPRAGE) image was acquired with the following parameters: TR = 1810 ms; TE = 3.5 ms; TI = 1100 ms, FOV = 180 × 240 mm^2, matrix = 192 × 256, effective voxel resolution = 0.938 × 0.938 × 1 mm^3. Resting-state fMRI scans were acquired with a single-shot, interleaved multi-slice, gradient-echo, echo planar imaging (GE-EPI) sequence sensitive to BOLD contrast with the following parameters: TR = 3000 ms; TE = 32 ms; flip angle = 90°; FOV = 192 × 192 mm^2; matrix = 64 × 64; 46 slices; slice thickness/gap = 3/0 mm, effective voxel resolution = 3.0 × 3.0 × 3.0 mm^3. Resting-state scans consisted of 124 volumes. In addition, a B0 field map was derived for application of distortion correction procedures, using a double-echo, gradient-recalled echo (GRE) sequence: TR = 1000 ms; TE_1 = 2.69 ms; TE_2 = 5.27 ms; 44 slices; slice thickness/gap = 4/0 mm; FOV = 240 mm; effective voxel resolution = 3.75 × 3.75 × 4 mm^3.

2.5. Image processing

Before the processing of both structural and functional data, a custom adolescent template was created with Advanced Normalization Tools (ANTs; Avants and Gee, 2004; Avants et al., 2011a). The template was created to minimize registration bias and maximize sensitivity to detect regional effects that can be impacted by registration error (Avants et al., 2011a). Structural images were then processed and registered to this template using the ANTs cortical thickness pipeline (Tustison et al., 2014). This procedure includes brain extraction, N4 bias field correction (Tustison et al., 2010), Atropos probabilistic tissue segmentation (Avants et al., 2011b), and the SyN diffeomorphic registration method (Avants et al., 2008; Klein et al., 2009).

The fMRI data were processed with an empirically validated preprocessing pipeline implemented in the eXtensible Connectivity Pipeline (XCP) Engine (Ciric et al., 2018). Resting-state time series preprocessing included correction of distortion induced by magnetic field inhomogeneity using FMRIB Software Library (FSL)'s FUGUE utility (Jenkinson, 2003), realignment of all volumes to a selected reference volume using MCFLIRT (Jenkinson et al., 2002), interpolation of intensity outliers in each voxel's time series using AFNI's 3dDespike utility and demeaning and removal of first- and second-order trends. After the despiking and detrending, the functional data were de-noised using a 36-parameter confound regression model that has been shown to minimize associations with motion artifact and other nuisance variables (Ciric et al., 2017). Specifically, the confound regression model included the six framewise estimates of motion, the mean signal extracted from eroded white matter and cerebrospinal fluid compartments, the global signal, the derivatives of each of these nine parameters, and quadratic terms of each of the nine parameters as well as their derivatives. To avoid frequency mismatch, both the BOLD-weighted time series and the confound regressor timeseries were temporally filtered simultaneously using a first-order Butterworth filter with a passband between 0.01 and 0.08 Hz (Hallquist et al., 2013). Confound regression was performed using AFNI's 3dTproject. Denoised functional images were co-registered to the T1 image using boundary-based registration (Greve and Fischl, 2009) and aligned to the study-specific adolescent template using the ANTs transform for the T1 image as above. Functional images were resampled to 4 mm^3 isotropic voxels in the template space before CWAS for computational feasibility (Shehzad et al., 2014). However, higher spatial resolution images (2 mm^3) were used for follow-up seed-based analyses. Throughout, all transformations were concatenated so that only one interpolation was performed.

2.6. Image quality assurance

Some participants were excluded due to inadequate structural image quality (n = 3), as determined by three expert raters (Rosen et al., 2018). As described in prior work (Satterthwaite et al., 2013; Ciric et al., 2018), a participant's resting-state fMRI data was excluded if the mean relative root mean square (RMS) framewise displacement was higher than 0.2 mm, or if it had more than 20 frames with motion exceeding 0.25 mm (n = 133). One participant was also excluded when manual inspection revealed fewer data points than expected in the resting-state scan (n = 1). Our final sample thus included 293 participants. Additionally, to account for residual motion in the data that passed quality assurance, we included RMS framewise displacement as a covariate in all models.

2.7. Multivariate distance-based matrix regression (MDMR)

We conducted a connectome-wide analysis using MDMR as described in detail in previous studies (Shehzad et al., 2014; Satterthwaite et al., 2015; Sharma et al., 2017) with the goal of understanding how the temporal discounting rate was associated with individual differences in the multivariate pattern of FC at each voxel. Matrix regression is a class of statistical methods that have been widely used in genomics and ecology research (Minas and Montana, 2014; Zakharov et al., 2013) and have been increasingly used for analysis of high-dimensional imaging data (Chen et al., 2022; Kim et al., 2022; Bolt et al., 2019). In this approach, the outcome of the regression equation is not a single vector of values, but rather a distance matrix between participants (see Fig. 1). Here we constructed a distance matrix for each location in the brain, using the connectivity of a specific voxel to the rest of the brain for each participant. Thus, we generated a unique distance matrix and ran a separate matrix regression for each voxel, with the distance matrix as the outcome; predictor variables included log(k), age, sex, and in-scanner motion.

A schematic of the CWAS procedure is depicted in Fig. 1. First, the preprocessed participant BOLD time series were used to conduct seed-based connectivity analyses at each voxel within gray matter. Specifically, Pearson's correlation coefficient between each voxel's time series and the time series of every other gray matter voxel (Fig. 1**A & B**) was used to generate subject-level connectivity maps. Second, we summarized individual differences in FC maps by computing a distance matrix (also using Pearson's correlation) between the connectivity matrices for every possible pairing of participants (Fig. 1**C**). Third, MDMR (Fig. 1**D**) was used to test how well our phenotypic variable, log(k), explained variation in the distances between connectivity matrices across participants. This approach provided a measure of how FC patterns across participants were impacted by individual differences in log(k), while controlling for the effects of age, sex (assigned at birth), and in-scanner motion (Shehzad et al., 2014; Satterthwaite et al., 2015). MDMR yields a pseudo-F statistic for each voxel, whose significance is assessed using 5000 iterations of a permutation test to generate a null distribution. The ultimate product of this procedure was a voxel-wise z-statistic map describing the association between log(k) and the global pattern of connectivity for each voxel (Fig. 1**E**). Aligning with current recommendations to minimize false positives, the type I error rate across voxels was controlled using cluster correction with a voxel height of $z > 3.09$ and utilized a cluster-extent probability threshold $p < 0.05$ (Eklund et al., 2016). We also ran an analysis to explore interactions with age and sex (log(k)*age or log(k)*sex); these models included the

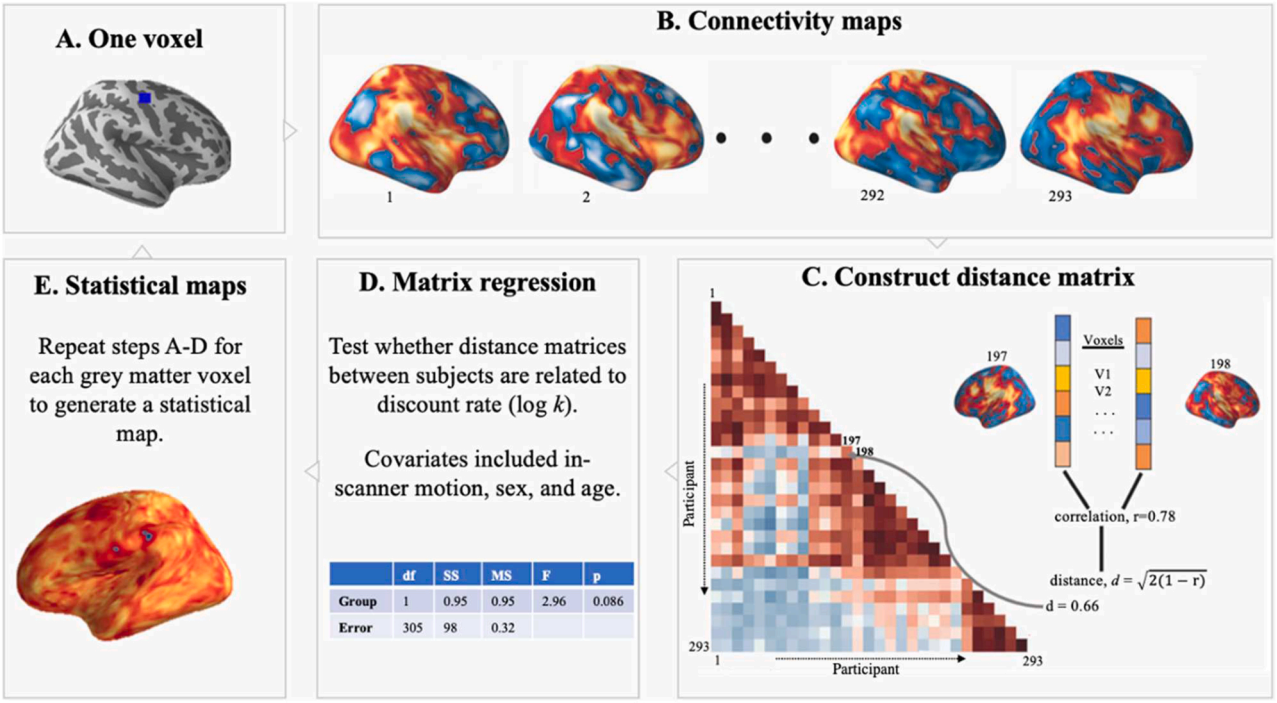

Fig. 1. Connectome-wide analysis approach. For each gray matter voxel (**A**), a connectivity map was created for each subject (**B**), and the maps were compared in a pairwise manner (using correlation) to create a participant-by-participant distance matrix (**C**). Multivariate distance-based matrix regression (MDMR) was used to evaluate how the multivariate patterns of connectivity encoded by these distance matrices were associated with individual differences in delay discounting while controlling for age, sex, and in-scanner motion (**D**). Permutation testing yielded a pseudo-*F* statistic and a corresponding *p* value. This procedure was repeated for each gray matter voxel, yielding a voxel-wise statistical map (**E**).

same covariates listed above.

2.8. Seed-based analyses

MDMR identified clusters where the overall multivariate pattern of connectivity is dimensionally related to DD, but it did not describe the specific pairwise FC patterns that drove the multivariate results. To characterize the direction of the effects, as in previous studies (Satterthwaite et al., 2015; Sharma et al., 2017), we conducted post-hoc seed-based descriptive analyses for each cluster returned by MDMR. Group-level seed analysis included age, sex, and in-scanner motion as covariates and was computed using a general linear model (implemented in FSL's *flameo*; Woolrich et al., 2004). These follow-up analyses were descriptive, as the seeds were selected based on the significance of the MDMR result.

2.9. Network enrichment testing

Given that neural activity differs across functional networks (Raut et al., 2020), we attempted to localize effects of interest within specific brain networks during rest. Specifically, we examined whether associations with log(k) revealed by the seed-based analyses described above were located within one of the seven canonical large-scale brain networks (Yeo et al., 2011) using a conservative network enrichment testing procedure (see Baller et al., 2022 for details). To account for the different size of each network and the spatial autocorrelation of brain maps, statistical testing used a conservative spin-based spatial permutation procedure (Alexander-Bloch et al., 2018). Areas with positive and negative associations were evaluated separately. Briefly, statistical maps from the seed-based analysis were thresholded at $|z| \geq 3.09$ and projected onto a spherical representation of the cortical surface. This sphere was rotated 1000 times per hemisphere to create a null distribution. For both the real and permuted data, we evaluated proportion of vertices that overlapped with each of the seven canonical functional networks. Networks were considered to have significant enrichment if the test statistic in the observed data was in the top 5 % of the null distribution derived from permuted data.

2.10. Sensitivity analyses

To probe whether our results could be driven by individual differences in socioeconomic status (SES), mean parental education was included as a model covariate in addition to age, sex, and head motion. The average of mean parental years of education was 14.24 with a standard deviation of 2.21. We also ran a separate model including degree of model fit of the delay discounting data as a covariate. We performed an additional analysis that included overall psychopathology as measured by a structured clinical interview as a covariate to evaluate if overall mental health impacted results (Shanmugan et al., 2016). Similarly, we additionally examined if covarying for overall accuracy on a computerized cognitive battery impacted results (Moore et al., 2015).

3. Results

3.1. Connectome-wide analyses identify a region of connectivity related to DD

We sought to determine whether and how individual differences in DD were associated with complex, multivariate patterns of FC in a large sample of children, adolescents, and adults. Notably, we found no significant correlation between log(k) and either age or sex. However, as these variables may be strongly associated with FC, they were included as model covariates in the connectome-wide analysis.

Our connectome-wide analysis using MDMR revealed that DD was related to a multivariate pattern of FC in the left dorsal prefrontal cortex (dPFC; cluster center of gravity: x = 30.9, y = 43.8, z = 30.3; k = 12 voxels, $p_{fwe} = 1.03 \times 10^{-4}$, maximum z-value = 3.54; Fig. 2). This finding suggested a pivotal role of the dPFC, a hub of the DMN (Alves

Fig. 2. Connectome-wide analyses reveal that multivariate patterns of connectivity in the dorsal prefrontal cortex are associated with delay discounting. Volumetric depiction of the dorsal prefrontal cortex cluster identified by multivariate distance-based matrix regression. This dorsal prefrontal cortex cluster survived correction for multiple comparisons at $z > 3.09$, $p < 0.05$.

et al., 2019; Andrews-Hanna et al., 2010), in DD-related activity. We additionally evaluated models that included interactions between DD and both sex and age; the interaction effects in these models were not statistically significant.

3.2. DD is related to individual differences in connectivity between attentional control and default mode networks

Having localized multivariate connectivity patterns associated with DD to the dPFC, we next sought to understand the individual differences in FC associated with DD that drove the observed MDMR results. We conducted seed-based connectivity analyses using the dPFC cluster identified by MDMR. In this general linear model, we included age, sex, and in-scanner motion as covariates. We first evaluated the mean pattern of connectivity for the dPFC cluster. Across the entire sample, the left dPFC seed was strongly connected to elements of the DMN, including the PCC and vmPFC. The seed was anticorrelated mainly to regions within the dorsal attention network (DAN), such as the inferior parietal lobule, and regions in the VAN such as the temporoparietal junction (Fig. 3). This connectivity profile suggests that the dPFC cluster was primarily affiliated with the DMN.

Next, we sought to determine how DD was associated with individual differences in FC from the dPFC seed identified by the connectome-wide analysis. Analysis of the cluster within the left dPFC revealed that higher rates of DD were correlated with increased connectivity between the dPFC and other elements of the DMN, including the PCC and lateral temporal cortex (Fig. 4). In contrast, higher levels of DD were correlated with lower connectivity between the dPFC and regions within the VAN (including the temporoparietal junction and parts of the ventral frontal cortex) and the DAN (including the inferior parietal lobule and angular gyrus).

We next used spin-based network enrichment testing to statistically evaluate the spatial distribution of these effects. Enrichment testing revealed an enrichment of positive associations with log(k) in the DMN ($p = 0.01$). In contrast, there was enrichment of negative associations in the DAN ($p = 2 \times 10^{-3}$) and VAN ($p = 1.5 \times 10^{-3}$). Together, these results could suggest that DD in children, adolescents, and adults is associated with individual differences in connectivity within the DMN and between the DMN and attention networks. Specifically, higher rates of discounting (more impulsive choices) are associated with greater

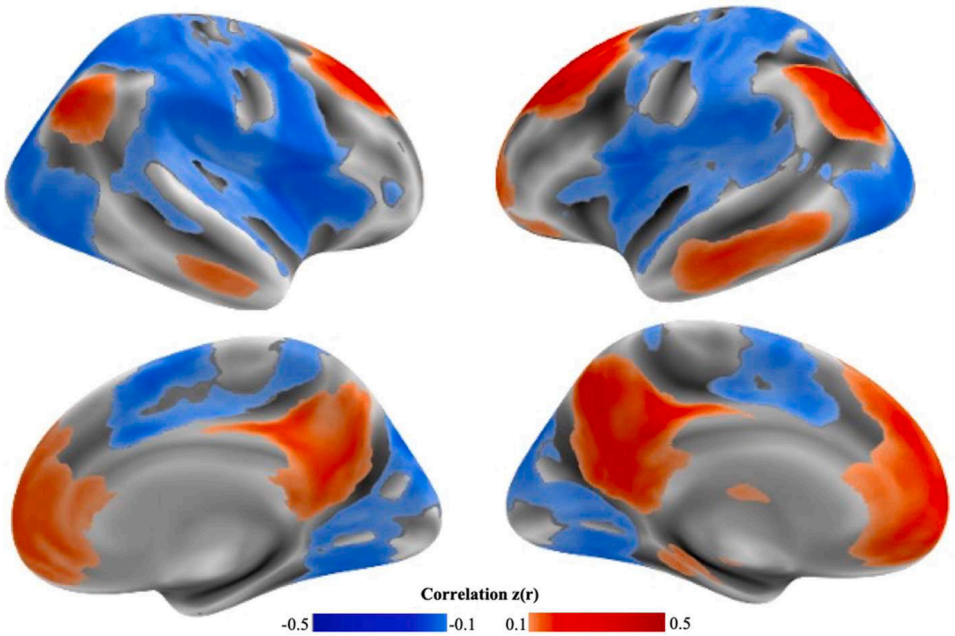

Fig. 3. Mean connectivity of the dorsal prefrontal cortex cluster. The cluster identified by the connectome-wide association study (see Fig. 2) was used as a seed to understand the connectivity profiles of the regions related to delay discounting. The left dorsal prefrontal cortex cluster had robust connectivity to other elements of the default mode network and was anticorrelated primarily with the dorsal and ventral attention network regions.

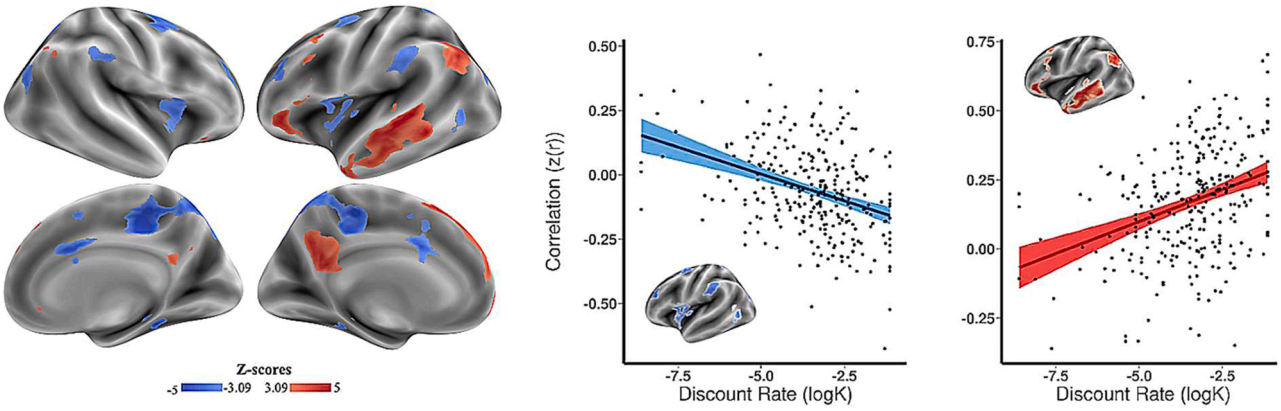

Fig. 4. Individual differences in delay discounting are associated with dorsal prefrontal cortex connectivity to the default mode network, as well as control and attention networks. Follow-up seed-based analyses from the dorsal prefrontal cortex revealed that increased discount rate was associated primarily with increased connectivity with other elements of the default mode network (red), as well as diminished connectivity with mainly the dorsal and ventral attention network regions (blue). Maps represent patterns that drove the connectome-wide association study result rather than independent statistical tests. The maps are thresholded for display at $|z| > 3.09$, $p < 0.05$.

connectivity between the dPFC and other DMN regions, but lower connectivity between the dPFC and attentional control regions.

3.3. Sensitivity analyses

The dPFC cluster remained significant in the same location when SES was added as a model covariate as part of sensitivity analyses. A significant cluster remained in the dPFC when overall psychopathology (p_{fwe}= 0.01) or overall cognitive performance were included as model covariates (p_{fwe}= 0.01). Finally, after including degree of model fit of the discount function as an additional covariate, a significant cluster (p_{fwe}= 0.01) remained in the dPFC.

4. Discussion

In this study, we used a data-driven approach to identify multivariate FC patterns that underlie DD in a large sample of children, adolescents, and adults. Our approach revealed that connectivity patterns of a region within the DMN—the dPFC—related to individual differences in DD. Further analyses revealed that higher DD was associated with increased FC of the dPFC with other regions within the DMN, and reduced FC with regions within the DAN and VAN. Taken together, these findings suggest that the dPFC may be a key node important for individual differences in impulsive choice within large-scale functional networks during resting-state imaging.

Notably, different parts of the dPFC are related to different aspects of DD, including the dlPFC, an executive control region, (Hare et al., 2014) and the dMPFC, implicated in processing future rewards and delay time (Wang et al., 2021). The dmPFC is considered a pivotal part of the DMN (Andrews-Hanna et al., 2010), and is thought to function in one of three subsystems within the DMN (Qi et al., 2018; Zhu et al., 2017; Tozzi et al., 2021). In particular, the dmPFC subsystem has been implicated in theory of mind and morality judgments (Broulidakis et al., 2016). A similar perspective-taking process might be involved in attributing value to one's own outcomes in the future; consistent with this possibility, suppression of a different node of the dmPFC subsystem increases DD (Soutschek et al., 2020). Other regions of the DMN, including the vmPFC and PCC, have been implicated in subjective valuation processes critical for decision-making (Pfeifer and Berkman, 2018; Bartra et al., 2013; Kable and Glimcher, 2007). Greater impulsivity has been associated with changes in how these regions represent reward features and value differences during DD tasks (Vanyukov et al., 2016; Koban et al., 2023). When interpreted in the context of these previous findings, our results suggest that stronger integration between the dPFC and other hubs of the DMN involved in valuation could be associated with impulsive decision-making, consistent with at least one smaller study in younger adults (Jung, 2021). It should be noted that since other regions within the DMN, such as the vmPFC (Bartra et al., 2013) have also been associated with DD processes previously, it is possible that this connectivity was obscured by the lower signal-to-noise ratio in the vmPFC. The cluster identified is also well-placed to mediate connectivity between other regions involved in DD and the vmPFC.

We found that participants with a greater discount rate also showed greater anticorrelation between the dPFC and networks involved in attentional and cognitive control such as the DAN and VAN during rest. This pattern mirrors resting-state functional segregation—or increased anticorrelation between disparate brain networks (Fair et al., 2007). Our results parallel previous studies showing that resting-state functional segregation between large-scale networks—for example, the connectivity of the DMN with the cingulo-opercular network, which is involved in cognitive control (Sadaghiani and D'Esposito, 2015)—can predict DD (Chen et al., 2018). This pattern of anticorrelation with the attention networks aligns with the frequently observed dissociation between task-positive attention networks and the task-negative DMN at rest (Fox et al., 2005). These findings suggest that stronger connections between regions within the DMN, together with weaker connections between the DMN and attentional control networks, could underlie higher DD through changes in attentional control and reward valuation.

Prior work suggests that adolescence is an important period for the general organization of large-scale FC, in which changes in connectivity adhere to a sensorimotor-association gradient that culminates in the DMN, a network clearly implicated in our analyses (Sydnor et al., 2023; Margulies et al., 2016). Further, the FC of the dPFC is known to evolve throughout adolescence with a shift from general to more differentiated abilities (Li et al., 2022). There is also evidence for functional separation between regions of the dPFC including the dmPFC and dlPFC, both regions involved in DD (Li et al., 2022). Nonetheless, we found no associations between age and DD in our work.

4.1. Limitations

Several limitations of this work should be noted. First, our study is cross-sectional rather than longitudinal, which may have limited our ability to find associations between age and DD. However, the null effects seen in our sample do align with the inconsistent and small age effects in the DD literature as noted before (Romer et al., 2017). Nonetheless, it is important to acknowledge that developmental changes in DD may occur at earlier ages than those studied here, and that

longitudinal studies might detect developmental effects through measurement of within-person change documented in previous studies (Anandakumar et al., 2018; Achterberg et al., 2016). Further, we only considered one measure of impulsive choice. While the discount rate is a standard measure of temporal discounting, there are other analytic approaches that attempt to decompose the contributions of amount sensitivity and delay sensitivity (see de Water et al., 2017). It is possible that some of these other variables are sensitive to developmental changes in impulsive behavior. For example, time before first move on the Tower of London task, which could be considered an index of impulsivity, is associated with development (Steinberg et al., 2008). Future work should consider multiple measures of impulsivity.

Second, the MDMR approach has limited sensitivity in many settings, potentially increasing the risk of type II error. For example, MDMR analysis is often insensitive to more focal changes because it summarizes differences in distributed multivariate patterns of connectivity (Misaki et al., 2018). Finally, our task used hypothetical rather than real rewards as part of the DD paradigm. However, previous research has not revealed differences between performance on DD tasks with real versus hypothetical rewards (Bickel et al., 2009).

4.2. Conclusions

We found that the pattern of dPFC connectivity is related to individual differences in impulsive choice during childhood, adolescence and adulthood. Multivariate patterns associated with impulsive choice were driven primarily by increased connectivity between the dPFC and other parts of the DMN, as well as diminished connectivity with attention networks at rest. Moving forward, the results from this data-driven analysis will be important to replicate. While speculative, these results also suggest that the dPFC may be a potential target for TMS and neuromodulatory therapies for conditions where impulsivity is prominent.

Declaration of Competing Interest

The authors declare that they have no known competing financial interests or personal relationships that could have appeared to influence the work reported in this paper.

Data availability

The Philadelphia Neurodevelopmental Cohort is a publicly available dataset at https://www.ncbi.nlm.nih.gov/projects/gap/cgi-bin/study.cgi?study_id=phs000607.v3.p2.

All code and a reproducibility guide for this project is available at https://github.com/PennLINC/pncitc.

Acknowledgements

This work was supported by the U.S. National Institute of Mental Health (U.S.A) MH120174 (David R. Roalf), MH119185 (David R. Roalf), R01MH117014 (Ruben C. Gur, Raquel E. Gur), R01MH119219 (Ruben C. Gur, Raquel E. Gur), R01MH120482 (Theodore D. Satterthwaite), R01MH113550 (Theodore D. Satterthwaite), R01EB022573 (Theodore D. Satterthwaite), R37MH125829 (Theodore D. Satterthwaite), RC2MH089983 (Raquel E. Gur), RC2MH089924 (Raquel E. Gur), T32MH014654 (Bart Larsen), K99MH127293 (Bart Larsen), K23MH133118 (Erica B. Baller), T32MH019112 (Erica B. Baller), R01MH113565 (Daniel H. Wolf), F31MH123063 (Adam Pines), and Deutsche Forschungsgemeinschaft (Germany) 269953372/GRK2150 (Martin Gell); additional support was provided by the Penn-CHOP Lifespan Brain Institute. There are no competing interests at this time.

Appendix A. Supporting information

Supplementary data associated with this article can be found in the online version at doi:10.1016/j.dcn.2023.101265.

References

Achterberg, M., Peper, J.S., Duijvenvoorde, A.C.K., van, Mandl, R.C.W., Crone, E.A., 2016. Frontostriatal white matter integrity predicts development of delay of gratification: a longitudinal study. J. Neurosci. 36 (6), 1954–1961. https://doi.org/10.1523/JNEUROSCI.3459-15.2016.

Alexander-Bloch, A., Shou, H., Liu, S., Satterthwaite, T.D., Glahn, D.C., Shinohara, R.T., Vandekar, S.N., Raznahan, A., 2018. On testing for spatial correspondence between maps of human brain structure and function. Neuroimage 178, 540–551. https://doi.org/10.1016/j.neuroimage.2018.05.070.

Alves, P.N., Foulon, C., Karolis, V., Bzdok, D., Margulies, D.S., Volle, E., Thiebaut de Schotten, M., 2019. An improved neuroanatomical model of the default-mode network reconciles previous neuroimaging and neuropathological findings. Article 1 Commun. Biol. 2 (1). https://doi.org/10.1038/s42003-019-0611-3.

Amlung, M., Marsden, E., Holshausen, K., Morris, V., Patel, H., Vedelago, L., Naish, K.R., Reed, D.D., McCabe, R.E., 2019. Delay discounting as a transdiagnostic process in psychiatric disorders: a meta-analysis. JAMA Psychiatry 76 (11), 1176–1186. https://doi.org/10.1001/jamapsychiatry.2019.2102.

Anandakumar, J., Mills, K.L., Earl, E.A., Irwin, L., Miranda-Dominguez, O., Demeter, D. V., Walton-Weston, A., Karalunas, S., Nigg, J., Fair, D.A., 2018. Individual differences in functional brain connectivity predict temporal discounting preference in the transition to adolescence. Dev. Cogn. Neurosci. *34*. https://doi.org/10.1016/j.dcn.2018.07.003.

Andrews-Hanna, J.R., Reidler, J.S., Sepulcre, J., Poulin, R., Buckner, R.L., 2010. Functional-anatomic fractionation of the brain's default network. Neuron 65 (4), 550–562. https://doi.org/10.1016/j.neuron.2010.02.005.

Avants, B., Gee, J.C., 2004. Geodesic estimation for large deformation anatomical shape averaging and interpolation. NeuroImage 23 (Suppl 1). https://doi.org/10.1016/j.neuroimage.2004.07.010.

Avants, B.B., Tustison, N.J., Song, G., Cook, P.A., Klein, A., Gee, J.C. (2011a). A reproducible evaluation of ANTs similarity metric performance in brain image registration—PubMed.

Avants, B.B., Epstein, C.L., Grossman, M., Gee, J.C., 2008. Symmetric diffeomorphic image registration with cross-correlation: evaluating automated labeling of elderly and neurodegenerative brain. Med. Image Anal. 12 (1), 26–41. https://doi.org/10.1016/j.media.2007.06.004.

Avants, B.B., Tustison, N.J., Wu, J., Cook, P.A., Gee, J.C., 2011b. An open source multivariate framework for n-tissue segmentation with evaluation on public data. Neuroinformatics 9 (4). https://doi.org/10.1007/s12021-011-9109-y.

Baller, E.B., Valcarcel, A.M., Adebimpe, A., Alexander-Bloch, A., Cui, Z., Gur, R.C., Gur, R.E., Larsen, B.L., Linn, K.A., O'Donnell, C.M., Pines, A.R., Raznahan, A., Roalf, D.R., Sydnor, V.J., Tapera, T.M., Tisdall, M.D., Vandekar, S., Xia, C.H., Detre, J.A., Shinohara, R.T., Satterthwaite, T.D., 2022. Developmental coupling of cerebral blood flow and fMRI fluctuations in youth. Cell Rep. 38 (13), 110576.

Bartra, O., McGuire, J.T., Kable, J.W., 2013. The valuation system: a coordinate-based meta-analysis of BOLD fMRI experiments examining neural correlates of subjective value. NeuroImage *76*. https://doi.org/10.1016/j.neuroimage.2013.02.063.

Bickel, W.K., Pitcock, J.A., Yi, R., Angtuaco, E.J.C., 2009. Congruence of BOLD response across intertemporal choice conditions: fictive and real money gains and losses. J. Neurosci. 29 (27), 8839–8846. https://doi.org/10.1523/JNEUROSCI.5319-08.2009.

Bickel, W.K., Jarmolowicz, D.P., Mueller, E.T., Koffarnus, M.N., Gatchalian, K.M., 2012. Excessive discounting of delayed reinforcers as a trans-disease process contributing to addiction and other disease-related vulnerabilities: emerging evidence. Pharmacol. Ther. 134 (3), 287. https://doi.org/10.1016/j.pharmthera.2012.02.004.

Bolt, T., Nomi, J.S., Bainter, S.A., Cole, M.W., Uddin, L.Q., 2019. The situation or the person? Individual and task-evoked differences in BOLD activity. Hum. Brain Mapp. 40 (10), 2943–2954. https://doi.org/10.1002/hbm.24570.

Broulidakis, M.J., Fairchild, G., Sully, K., Blumensath, T., Darekar, A., Sonuga-Barke, E.J. S., 2016. Reduced default mode connectivity in adolescents with conduct disorder. e1 J. Am. Acad. Child Adolesc. Psychiatry 55 (9), 800–808. https://doi.org/10.1016/j.jaac.2016.05.021.

Button, K., Ioannidis, J., Mokrysz, C., et al., 2013. Power failure: why small sample size undermines the reliability of neuroscience. Nat. Rev. Neurosci. 14, 365–376. https://doi.org/10.1038/nrn3475.

Calluso, C., Tosoni, A., Pezzulo, G., Spadone, S., Committeri, G., 2015. Interindividual variability in functional connectivity as long-term correlate of temporal discounting. PLOS ONE 10 (3), e0119710. https://doi.org/10.1371/journal.pone.0119710.

Chase, H.W., Hogarth, L., 2011. Impulsivity and symptoms of nicotine dependence in a young adult population. Nicotine Tob. Res. 13 (12), 1321–1325. https://doi.org/10.1093/ntr/ntr114.

Chen, A.A., Srinivasan, D., Pomponio, R., Fan, Y., Nasrallah, I.M., Resnick, S.M., Beason-Held, L.L., Davatzikos, C., Satterthwaite, T.D., Bassett, D.S., Shinohara, R.T., Shou, H., 2022. Harmonizing functional connectivity reduces scanner effects in community detection. NeuroImage 256, 119198. https://doi.org/10.1016/j.neuroimage.2022.119198.

Chen, Z., Guo, Y., Feng, T., 2017. Delay discounting is predicted by scale-free dynamics of default mode network and salience network. Neuroscience 362, 219–227. https://doi.org/10.1016/j.neuroscience.2017.08.028.

Chen, Z., Guo, Y., Suo, T., Feng, T., 2018. Coupling and segregation of large-scale brain networks predict individual differences in delay discounting. Biol. Psychol. *133*. https://doi.org/10.1016/j.biopsycho.2018.01.011.

Ciric, R., Wolf, D.H., Power, J.D., Roalf, D.R., Baum, G.L., Ruparel, K., Shinohara, R.T., Elliott, M.A., Eickhoff, S.B., Davatzikos, C., Gur, R.C., Gur, R.E., Bassett, D.S., Satterthwaite, T.S., 2017. Benchmarking of participant-level confound regression strategies for the control of motion artifact in studies of functional connectivity. NeuroImage. https://doi.org/10.1016/j.neuroimage.2017.03.020.

Ciric, R., Rosen, A.F.G., Erus, G., Cieslak, M., Adebimpe, A., Cook, P.A., Bassett, D.S., Davatzikos, C., Wolf, D.H., Satterthwaite, T.D., 2018. Mitigating head motion artifact in functional connectivity MRI. Nat. Protoc. 13 (12) https://doi.org/10.1038/s41596-018-0065-y.

Costa Dias, T.G., Wilson, V.B., Bathula, D.R., Iyer, S.P., Mills, K.L., Thurlow, B.L., Stevens, C.A., Musser, E.D., Carpenter, S.D., Grayson, D.S., Mitchell, S.H., Nigg, J.T., Fair, D.A., 2013. Reward circuit connectivity relates to delay discounting in children with attention-deficit/hyperactivity disorder. Eur. Neuropsychopharmacol.: J. Eur. Coll. Neuropsychopharmacol. 23 (1), 33–45. https://doi.org/10.1016/j.euroneuro.2012.10.015.

Eklund, A., Nichols, T.E., Knutsson, H., 2016. Cluster failure: why fMRI inferences for spatial extent have inflated false-positive rates. *PNAS*.

Epstein, L.H., Salvy, S.J., Carr, K.A., Dearing, K.K., Bickel, W.K., 2010. Food reinforcement, delay discounting and obesity. Physiol. Behav. 100 (5), 438. https://doi.org/10.1016/j.physbeh.2010.04.029.

Fair, D.A., Dosenbach, N.U.F., Church, J.A., Cohen, A.L., Brahmbhatt, S., Miezin, F.M., Barch, D.M., Raichle, M.E., Petersen, S.E., Schlaggar, B.L., 2007. Development of distinct control networks through segregation and integration. Proc. Natl. Acad. Sci. 104 (33), 13507–13512. https://doi.org/10.1073/pnas.0705843104.

Fox, M.D., Snyder, A.Z., Vincent, J.L., Corbetta, M., Van Essen, D.C., Raichle, M.E., 2005. The human brain is intrinsically organized into dynamic, anticorrelated functional networks. Proc. Natl. Acad. Sci. 102 (27), 9673–9678. https://doi.org/10.1073/pnas.0504136102.

Greve, D.N., Fischl, B., 2009. Accurate and robust brain image alignment using boundary-based registration. NeuroImage 48 (1). https://doi.org/10.1016/j.neuroimage.2009.06.060.

Gur, R.C., Richard, J., Hughett, P., Calkins, M.E., Macy, L., Bilker, W.B., Brensinger, C., Gur, R.E., 2010. A cognitive neuroscience-based computerized battery for efficient measurement of individual differences: standardization and initial construct validation. J. Neurosci. Methods 187 (2), 254–262. https://doi.org/10.1016/j.jneumeth.2009.11.017.

Gur, R.C., Richard, J., Calkins, M.E., Chiavacci, R., Hansen, J.A., Bilker, W.B., Loughead, J., Connolly, J.J., Qiu, H., Mentch, F.D., Abou-Sleiman, P.M., Hakonarson, H., Gur, R.E., 2012. Age group and sex differences in performance on a computerized neurocognitive battery in children age 8-21. Neuropsychology 26 (2), 251–265. https://doi.org/10.1037/a0026712.

Hallquist, M.N., Hwang, K., Luna, B., 2013. The nuisance of nuisance regression: Spectral misspecification in a common approach to resting-state fMRI preprocessing reintroduces noise and obscures functional connectivity. NeuroImage *82*. https://doi.org/10.1016/j.neuroimage.2013.05.116.

Hare, T.A., Hakimi, S., Rangel, A., 2014. Activity in dlPFC and its effective connectivity to vmPFC are associated with temporal discounting. Front. Neurosci. *0*. https://doi.org/10.3389/fnins.2014.00050.

Hirsh, J.B., Morisano, D., Peterson, J.B., 2008. Delay discounting: interactions between personality and cognitive ability. J. Res. Personal. 42 (6), 1646–1650. https://doi.org/10.1016/j.jrp.2008.07.005.

Jenkinson, M., 2003. Fast, automated, N-dimensional phase-unwrapping algorithm. Magn. Reson. Med. 49 (1) https://doi.org/10.1002/mrm.10354.

Jenkinson, M., Bannister, P., Brady, M., Smith, S., 2002. Improved optimization for the robust and accurate linear registration and motion correction of brain images. NeuroImage 17 (2). https://doi.org/10.1016/s1053-8119(02)91132-8.

Jung, W.H., 2021. Individual differences of functional brain networks from resting-state fMRI and delay discount rate. Korean J. Cogn. Biol. Psychol. 33 (1), 15–29. https://doi.org/10.22172/cogbio.2021.33.1.002.

Kable, J.W., Glimcher, P.W., 2007. The neural correlates of subjective value during intertemporal choice. Nat. Neurosci. 10 (12) https://doi.org/10.1038/nn2007.

Kable, J.W., Glimcher, P.W., 2010. An "as soon as possible" effect in human intertemporal decision making: Behavioral evidence and neural mechanisms. J. Neurophysiol. 103 (5) https://doi.org/10.1152/jn.00177.2009.

Kable, J.W., Levy, I., 2015. Neural markers of individual differences in decision-making. Curr. Opin. Behav. Sci. 5, 100. https://doi.org/10.1016/j.cobeha.2015.08.004.

Kim, M.J., Elliott, M.L., Knodt, A.R., Hariri, A.R., 2022. A connectome-wide functional signature of trait anger. Clin. Psychol. Sci.: A J. Assoc. Psychol. Sci. 10 (3), 584–592. https://doi.org/10.1177/21677026211030240.

Kirby, K.N., 2009. One-year temporal stability of delay-discount rates. Psychon. Bull. Rev. 16 (3), 457–462. https://doi.org/10.3758/PBR.16.3.457.

Klein, A., Andersson, J., Ardekani, B.A., Ashburner, J., Avants, B., Chiang, M.C., Christensen, G.E., Collins, D. l, Gee, J., Hellier, P., Song, J.H., Jenkinson, M., Lepage, C., Rueckert, D., Thompson, P., Vercauteren, T., Woods, R.P., Mann, J.J., R. V, P., 2009. Evaluation of 14 nonlinear deformation algorithms applied to human brain MRI registration. NeuroImage 46 (3). https://doi.org/10.1016/j.neuroimage.2008.12.037.

Koban, L., Lee, S., Schelski, D.S., Simon, M.C., Lerman, C., Weber, B., Kable, J.W., Plassmann, H., 2023. An fMRI-based brain marker of individual differences in delay discounting. J. Neurosci. 43 (9), 1600–1613.

Lempert, K.M., Steinglass, J.E., Pinto, A., Kable, J.W., Simpson, H.B., 2019. Can delay discounting deliver on the promise of RDoC? Psychol. Med. 49 (2), 190–199. https://doi.org/10.1017/S0033291718001770.

Li, N., Ma, N., Liu, Y., He, X.-S., Sun, D.-L., Fu, X.-M., Zhang, X., Han, S., Zhang, D.-R., 2013. Resting-state functional connectivity predicts impulsivity in economic decision-making. J. Neurosci. 33 (11), 4886–4895. https://doi.org/10.1523/JNEUROSCI.1342-12.2013.

Li, W., Shi, W., Wang, H., Li, J., Cui, Y., Li, K., Cheng, L., Lu, Y., Ma, L., Chu, C., Song, M., Yang, Z., Banaschewski, T., Bokde, A.L.W., Desrivières, S., Flor, H., Grigis, A., Garavan, H., Gowland, P., … Consortium, I. (2022). Anatomical connectivity profile development constrains medial-lateral topography in the dorsal prefrontal cortex (p. 2022.02.07.479322). bioRxiv. https://doi.org/10.1101/2022.02.07.479322.

Madden, G.J., Begotka, A.M., Raiff, B.R., Kastern, L.L., 2003. Delay discounting of real and hypothetical rewards. Exp. Clin. Psychopharmacol. 11 (2), 139–145. https://doi.org/10.1037/1064-1297.11.2.139.

Mahalingam, V., Palkovics, M., Kosinski, M., Cek, I., Stillwell, D., 2016. A computer adaptive measure of delay discounting. Assessment. https://doi.org/10.1177/1073191116680448.

Marek, S., Tervo-Clemmens, B., Calabro, F.J., Montez, D.F., Kay, B.P., Hatoum, A.S., Donohue, M.R., Foran, W., Miller, R.L., Hendrickson, T.J., Malone, S.M., Kandala, S., Feczko, E., Miranda-Dominguez, O., Graham, A.M., Earl, E.A., Perrone, A.J., Cordova, M., Doyle, O., Dosenbach, N.U.F., 2022. Reproducible brain-wide association studies require thousands of individuals. *Nat.*, *603*(7902), Artic. 7902. https://doi.org/10.1038/s41586-022-04492-9.

Margulies, D.S., Ghosh, S.S., Goulas, A., Falkiewicz, M., Huntenburg, J.M., Langs, G., Bezgin, G., Eickhoff, S.B., Castellanos, F.X., Petrides, M., Jefferies, E., Smallwood, J., 2016. Situating the default-mode network along a principal gradient of macroscale cortical organization. Proc. Natl. Acad. Sci. 113 (44), 12574–12579. https://doi.org/10.1073/pnas.1608282113.

Mazur, J.E., 1987. An adjusting procedure for studying delayed reinforcement. In: Commons, M.L., Mazur, J.E., Nevin, J.A. (Eds.), Quantitative analyses of behavior: the effect of delay and of intervening events on reinforcement value, Vol. 5. NJ: Lawrence Erlbaum, Hillsdale, pp. 55–73.

Minas, C., Montana, G., 2014. Distance-based analysis of variance: approximate inference. Stat. Anal. Data Min.: ASA Data Sci. J. 7 (6), 450–470. https://doi.org/10.1002/sam.11227.

Misaki, M., Phillips, R., Zotev, V., Wong, C.-K., Wurfel, B.E., Krueger, F., Feldner, M., Bodurka, J., 2018. Real-time fMRI amygdala neurofeedback positive emotional training normalized resting-state functional connectivity in combat veterans with and without PTSD: a connectome-wide investigation. NeuroImage: Clin. 20, 543. https://doi.org/10.1016/j.nicl.2018.08.025.

Mischel, W., Shoda, Y., Rodriguez, M.L., 1989. Delay of gratification in children. Science 244 (4907), 933–938. https://doi.org/10.1126/science.2658056.

Moore, T.M., Reise, S.P., Gur, R.E., Hakonarson, H., Gur, R.C., 2015. Psychometric properties of the Penn computerized neurocognitive battery. Neuropsychology 29, 235–246. https://doi.org/10.1037/neu0000093.

Ortiz, N., Parsons, A., Whelan, R., Brennan, K., Agan, M.L.F., O'Connell, R., Bramham, J., Laht, H., 2015. Decreased frontal, striatal and cerebellar activation in adults with ADHD during an adaptive delay discounting task. Acta Neurobiol. Exp. 75 (3), 326–338.

Pehlivanova, M., Wolf, D.H., Sotiras, A., Kaczkurkin, A.N., Moore, T.M., Ciric, R., Cook, P.A., Garza, A.G., de, L., Rosen, A.F.G., Ruparel, K., Sharma, A., Shinohara, R. T., Roalf, D.R., Gur, R.C., Davatzikos, C., Gur, R.E., Kable, J.W., Satterthwaite, T.D., 2018. Diminished cortical thickness is associated with impulsive choice in adolescence. J. Neurosci. 38 (10), 2471. https://doi.org/10.1523/JNEUROSCI.2200-17.2018.

Peters, J., Büchel, C., 2010. Episodic future thinking reduces reward delay discounting through an enhancement of prefrontal-mediotemporal interactions. Neuron 66 (1). https://doi.org/10.1016/j.neuron.2010.03.026.

Pfeifer, J.H., Berkman, E.T., 2018. The development of self and identity in adolescence: neural evidence and implications for a value-based choice perspective on motivated behavior. Child Dev. Perspect. 12 (3) https://doi.org/10.1111/cdep.12279.

Qi, H., Liu, H., Hu, H., He, H., Zhao, X., 2018. Primary disruption of the memory-related subsystems of the default mode network in Alzheimer's disease: resting-state functional connectivity MRI study. Front. Aging Neurosci. 10 https://www.frontiersin.org/articles/10.3389/fnagi.2018.00344.

Raut, R.V., Snyder, A.Z., Raichle, M.E., 2020. Hierarchical dynamics as a macroscopic organizing principle of the human brain. PNAS 117, 2089020897. https://doi.org/10.1073/pnas.2003383117.

Romer, D., Reyna, V.F., Satterthwaite, T.D., 2017. Beyond stereotypes of adolescent risk taking: placing the adolescent brain in developmental context. Dev. Cogn. Neurosci. 27, 19–34. https://doi.org/10.1016/j.dcn.2017.07.007.

Rosch, K.S., Mostofsky, S.H., Nebel, M.B., 2018. ADHD-related sex differences in fronto-subcortical intrinsic functional connectivity and associations with delay discounting. J. Neurodev. Disord. 10 (1), 34. https://doi.org/10.1186/s11689-018-9254-9.

Rosen, A.F.G., Roalf, D.R., Ruparel, K., Blake, J., Seelaus, K., Villa, L.P., Ciric, R., Cook, P. A., Davatzikos, C., Elliott, M.A., Garcia de La Garza, A., Gennatas, E.D., Quarmley, M., Schmitt, J.E., Shinohara, R.T., Tisdall, M.D., Craddock, R.C., Gur, R. E., Gur, R.C., Satterthwaite, T.D., 2018. Quantitative assessment of structural image quality. NeuroImage 169, 407–418. https://doi.org/10.1016/j.neuroimage.2017.12.059.

Sadaghiani, S., D'Esposito, M., 2015. Functional characterization of the cingulo-opercular network in the maintenance of tonic alertness. Cereb. Cortex 25 (9), 2763–2773. https://doi.org/10.1093/cercor/bhu072.

Satterthwaite, T.D., Elliott, M.A., Gerraty, R.T., Ruparel, K., Loughead, J., Calkins, M.E., Eickhoff, S.B., Hakonarson, H., Gur, R.C., Gur, R.E., Wolf, D.H., 2013. An improved framework for confound regression and filtering for control of motion artifact in the preprocessing of resting-state functional connectivity data. NeuroImage 64. https://doi.org/10.1016/j.neuroimage.2012.08.052.

Satterthwaite, T.D., Elliott, M.A., Ruparel, K., Loughead, J., Prabhakaran, K., Calkins, M. E., Hopson, R., Jackson, C., Keefe, J., Riley, M., Mensh, F.D., Sleiman, P., Verma, R.,

Davatzikos, C., Hakonarson, H., Gur, R.C., Gur, R.E., 2014. Neuroimaging of the Philadelphia neurodevelopmental cohort. NeuroImage 86, 544. https://doi.org/10.1016/j.neuroimage.2013.07.064.

Satterthwaite, T.D., Vandekar, S.N., Wolf, D.H., Bassett, D.S., Ruparel, K., Shehzad, Z., Craddock, R.C., Shinohara, R.T., Moore, T.M., Gennatas, E.D., Jackson, C., Roalf, D. R., Milham, M.P., Calkins, M.E., Hakonarson, H., Gur, R.C., Gur, R.E., 2015. Connectome-wide network analysis of youth with Psychosis-Spectrum symptoms. Mol. Psychiatry 20 (12). https://doi.org/10.1038/mp.2015.66.

Satterthwaite, T.D., Connolly, J.J., Ruparel, K., Calkins, M.E., Jackson, C., Elliott, Ma, Roalf, D.R., Hopson, R., Prabhakaran, K., Behr, M., Qiu, H., Mentch, F.D., Chiavacci, R., Sleiman, P.M.A., Gur, R.C., Hakonarson, H., Gur, R.E., 2016. The Philadelphia Neurodevelopmental Cohort: a publicly available resource for the study of normal and abnormal brain development in youth. NeuroImage 124 (Pt B). https://doi.org/10.1016/j.neuroimage.2015.03.056.

Schüller, C.B., Kuhn, J., Jessen, F., Hu, X., 2019. Neuronal correlates of delay discounting in healthy subjects and its implication for addiction: An ALE meta-analysis study. Am. J. Drug Alcohol Abus. https://doi.org/10.1080/00952990.2018.1557675.

Senecal, N., Wang, T., Thompson, E., Kable, J.W., 2012. Normative arguments from experts and peers reduce delay discounting. Judgm. Decis. Mak. 7 (5), 568. ⟨https://www.ncbi.nlm.nih.gov/pmc/articles/PMC3626281/⟩.

Shanmugan, S., Wolf, D.H., Calkins, M.E., Moore, T.M., Ruparel, K., Hopson, R.D., et al., 2016. Common and dissociable mechanisms of executive system dysfunction across psychiatric disorders in youth. Am. J. Psychiatry.

Sharma, A., Wolf, D.H., Ciric, R., Kable, J.W., Moore, T.M., Vandekar, S.N., Katchmar, N., Daldal, A., Ruparel, K., Davatzikos, C., Elliott, M.A., Calkins, M.E., Shinohara, R.T., Bassett, D.S., Satterthwaite, T.D., 2017. Connectome-wide analysis reveals common dimensional reward deficits across mood and psychotic disorders. Am. J. Psychiatry 174 (7), 657. https://doi.org/10.1176/appi.ajp.2016.16070774.

Shehzad, Z., Kelly, C., Reiss, P.T., Cameron Craddock, R., Emerson, J.W., McMahon, K., Copland, D.A., Castellanos, F.X., Milham, M.P., 2014. A multivariate distance-based analytic framework for connectome-wide association studies. NeuroImage 93 Pt 1 (0 1). https://doi.org/10.1016/j.neuroimage.2014.02.024.

Souther, M.K., Boateng, B., Kable, J.W., 2022. A meta-analysis of neural systems underlying delay discounting: Implications for transdiagnostic research. BioRxiv. https://doi.org/10.1101/2022.10.12.511959.

Soutschek, A., Moisa, M., Ruff, C.C., Tobler, P.N., 2020. The right temporoparietal junction enables delay of gratification by allowing decision makers to focus on future events. PLOS Biol. 18 (8), e3000800 https://doi.org/10.1371/journal.pbio.3000800.

Steinberg, L., Albert, D., Cauffman, E., Banich, M., Graham, S., Woolard, J., 2008. Age differences in sensation seeking and impulsivity as indexed by behavior and self-report: evidence for a dual systems model. Dev. Psychol. 44 (6), 1764–1778. https://doi.org/10.1037/a0012955.

Sydnor, V.J., Larsen, B., Seidlitz, J., Adebimpe, A., Alexander-Bloch, A.F., Bassett, D.S., Bertolero, M.A., Cieslak, M., Covitz, S., Fan, Y., Gur, R.E., Gur, R.C., Mackey, A.P., Moore, T.M., Roalf, D.R., Shinohara, R.T., Satterthwaite, T.D., 2023. Intrinsic activity development unfolds along a sensorimotor-association cortical axis in youth. Nat. Neurosci. 26 (4), 638–649. https://doi.org/10.1038/s41593-023-01282-y.

Tjur, T., 2009. Coefficients of determination in logistic regression models—a new proposal: the coefficient of discrimination. Am. Stat. 63, 366–372. https://doi.org/10.1198/tast.2009.08210.

Tozzi, L., Zhang, X., Chesnut, M., Holt-Gosselin, B., Ramirez, C.A., Williams, L.M., 2021. Reduced functional connectivity of default mode network subsystems in depression: meta-analytic evidence and relationship with trait rumination. NeuroImage: Clin. 30, 102570 https://doi.org/10.1016/j.nicl.2021.102570.

Tustison, N.J., Avants, B.B., Cook, P.A., Zheng, Y., Egan, A., Yushkevich, P.A., Gee, J.C., 2010. N4ITK: improved N3 bias correction. IEEE Trans. Med. Imaging 29 (6). https://doi.org/10.1109/TMI.2010.2046908.

Tustison, N.J., Pa, C., Klein, A., Song, G., Das, S.R., Duda, J.T., Kandel, B.M., Strien, N., van, Stone, J.R., Gee, J.C., Avants, B.B., 2014. Large-scale evaluation of ANTs and FreeSurfer cortical thickness measurements. NeuroImage *99*. https://doi.org/10.1016/j.neuroimage.2014.05.044.

Vanyukov, P.M., Szanto, K., Hallquist, M.N., Siegle, G.J., Reynolds 3rd, C.F., Forman, S. D., Aizenstein, H.J., Dombrovski, A.Y., 2016. Paralimbic and lateral prefrontal encoding of reward value during intertemporal choice in attempted suicide. Psychol. Med. 46 (2), 381–391. https://doi.org/10.1017/S0033291715001890.

Wang, Q., Wang, Y., Wang, P., Peng, M., Zhang, M., Zhu, Y., Wei, S., Chen, C., Chen, X., Luo, S., Bai, X., 2021. Neural representations of the amount and the delay time of reward in intertemporal decision making. Hum. Brain Mapp. 42 (11), 3450–3469. https://doi.org/10.1002/hbm.25445.

Wang, S., Zhou, M., Chen, T., Yang, X., Chen, G., Gong, Q., 2017. Delay discounting is associated with the fractional amplitude of low-frequency fluctuations and resting-state functional connectivity in late adolescence. Article 1 Sci. Rep. 7 (1). https://doi.org/10.1038/s41598-017-11109-z.

de Water, E., Mies, G.W., Figner, B., Yoncheva, Y., van den Bos, W., Castellanos, F.X., Cillessen, A.H.N., Scheres, A., 2017. Neural mechanisms of individual differences in temporal discounting of monetary and primary rewards in adolescents. NeuroImage 153, 198–210. https://doi.org/10.1016/j.neuroimage.2017.04.013.

Weller, R.E., Avsar, K.B., Cox, J.E., Reid, M.A., White, D.M., Lahti, A.C., 2014. Delay discounting and task performance consistency in patients with schizophrenia. Psychiatry Res. 215 (2), 286–293. https://doi.org/10.1016/j.psychres.2013.11.013.

Woolrich, M.W., Behrens, T.E., Beckmann, C.F., Jenkinson, M., Smith, S.M., 2004. Multilevel linear modelling for FMRI group analysis using Bayesian inference. NeuroImage 21 (4). https://doi.org/10.1016/j.neuroimage.2003.12.023.

Yeo, B.T., Krienen, F.M., Sepulcre, J., Sabuncu, M.R., Lashkari, D., Hollinshead, M., Roffman, J.L., Smoller, J.W., Zöllei, L., Polimeni, J.R., et al., 2011. The organization of the human cerebral cortex estimated by intrinsic functional connectivity. J. Neurophysiol. 106, 1125–1165. https://doi.org/10.1152/jn.00338.2011.

Zakharov, S., Salim, A., Thalamuthu, A., 2013. Comparison of similarity-based tests and pooling strategies for rare variants. BMC Genom. 14, 50.

Zhu, X., Zhu, Q., Shen, H., Liao, W., Yuan, F., 2017. Rumination and default mode network subsystems connectivity in first-episode, drug-naive young patients with major depressive disorder. Article 1 Sci. Rep. 7 (1). https://doi.org/10.1038/srep43105.